Journal of Luminescence 170 (2016) 364–368

Contents lists available at ScienceDirect

Journal of Luminescence

journal homepage: www.elsevier.com/locate/jlumin

Highly luminescent Eu^{3+}-doped benzenetricarboxylate based materials

Ivan G.N. Silva [a], Danilo Mustafa [a,*], Bruno Andreoli [a], Maria C.F.C. Felinto [b], Oscar L. Malta [c], Hermi F. Brito [a,*]

[a] Departamento de Química Fundamental, Instituto de Química da Universidade de São Paulo, Av. Prof. Lineu Prestes 748, São Paulo 05508-900, SP, Brazil
[b] Centro de Química do Meio Ambiente, Instituto de Pesquisas Energéticas e Nucleares, Av. Prof. Lineu Prestes 2242, São Paulo 05508-000, SP, Brazil
[c] Departamento de Química Fundamental, Universidade Federal de Pernambuco, Av. Prof. Moraes Rego, 1235, Recife 50670-90, PE, Brazil

ARTICLE INFO

Article history:
Received 20 January 2015
Received in revised form
27 April 2015
Accepted 28 April 2015
Available online 9 May 2015

Keywords:
Benzenetricarboxylate
Trimesic acid
Europium doping
Yttrium
Lutetium
Photoluminescence

ABSTRACT

[RE(TMA)] anhydrous complexes (RE^{3+}: Y, Gd and Lu) present high red emission intensity with a quantum efficiency (~45%) for the [Y(TMA):Eu^{3+}] complexes, due to the absence of non-radioactive decay pathways mediated by water molecules. The complexes were prepared in mild conditions. All the compounds are crystalline and thermostable up to 460 °C. Phosphorescence data of the complexes with Y, Gd and Lu show that the T_1 state of the TMA^{3-} anion has energy higher than the $^5D_0$ emitting level of the Eu^{3+} ion, indicating that the ligand can act as an intramolecular energy sensitizer. The photoluminescence properties of the doped materials were studied based on the excitation and emission spectra and luminescence decay curves. The experimental intensity parameters (Ω_λ), lifetimes (τ), radiative (A_{rad}) and non-radiative (A_{nrad}) decay rates were determined and discussed.

1. Introduction

In the last decades, complexes containing carboxylate ligands have been extensively used due to their great structural variety in producing materials with large range of chemical properties and applications such as selective markers for medical applications, magnetic materials, gas storage, drug delivery, *etc.* [1–4].

Rare earth (RE) ions are used in applications like catalyzers and permanent magnets in hybrid cars batteries [5,6]. In photonic science these ions are very important due to their wide range of emissions, from infrared to ultraviolet [7], for *e.g.* Nd^{3+}, Eu^{3+}, Gd^{3+}, Tb^{3+} and Tm^{3+} ions which emit in the infrared, red, ultraviolet, green and blue regions, respectively. Besides, RE ions are applied to electroluminescent materials, persistent phosphors, structural probes, luminescent markers, display panels, *etc.* [8–11].

The luminescent properties of RE^{3+} depend mostly on their unusual energy level structure. The atomic character of the 4f transitions is due to the shielding from the chemical environment by the filled 5s and 5p sub-shells [12]. The 4f intraconfigurational transitions are forbidden to first order by the Laporte rule. Therefore, to overcome the small absorptivity coefficients, luminescence sensitizers are used to absorb and transfer energy efficiently to the RE ions. This phenomenon is a key feature in design of luminescent materials [13].

The Y^{3+} ($4d^0$) and Lu^{3+} ($4f^{14}$) ions exhibit no luminescence originated from the 4f–4f transitions, Gd^{3+} ($4f^7$) ion have a large energy gap (~32,000 cm^{-1}) between the $^8S_{7/2}$ ground state and the first $^6P_{7/2}$ excited state. In the RE^{3+}–TMA (trimesic acid) complexes, the energy level of the first triplet state (T_1) of the ligand is around 24,000 cm^{-1}, which is above the emitting $^5D_0$ level of the Eu^{3+} ion (~17,000 cm^{-1}) [14], enabling the ligand-to-metal energy transfer, involving also the $^5D_2$ and $^5D_1$ levels.

The [RE(TMA)] complexes containing La^{3+} to Eu^{3+} ions have six water molecules and are anhydrous for compounds with Tb^{3+} to Lu^{3+} ions (including Y^{3+}). In addition, the Gd^{3+}-complexes can be obtained in both forms, this effect occurs due to the lanthanide contraction. Since the presence of water molecules causes luminescence quenching, the [RE(TMA)] (RE^{3+}: Y, Gd and Lu) complexes can be used as host matrices resulting in the [RE(TMA):Eu^{3+}] systems, showing higher luminescence efficiency compared to the hydrated complexes [14–17].

In this work the synthesis, characterization and optical properties of [RE(TMA):Eu^{3+}(*x* mol%)] compounds (RE^{3+}: Y, Gd and Lu; *x*: 0.1, 0.5, 1.0, and 5.0 mol%) are reported. These highly luminescent materials were prepared by a one-step synthesis in water. The materials were characterized by elemental analysis, infrared

* Corresponding authors. Tel.: +55 11 30913708; fax: +55 11 38155579.
E-mail addresses: dmustafa@iq.usp.br (D. Mustafa), hefbrito@iq.usp.br (H.F. Brito).

http://dx.doi.org/10.1016/j.jlumin.2015.04.047
0022-2313/

spectroscopy (FTIR), thermogravimetry (TG/DTG), X-ray powder diffraction (XRD) and scanning electron microscopy (SEM). The photoluminescence properties were studied based on the excitation and emission spectra, and luminescence decay lifetimes of the emitting $^5D_0$ level of the Eu^{3+} ion. The experimental intensity parameters (Ω_λ), $^5D_0$ lifetime, emission efficiency (η), radiative (A_{rad}) and non-radiative (A_{nrad}) decay rates and CIE color coordinates (x, y) were also determined.

2. Experimental section

The $RECl_3 \cdot (H_2O)_6$ were obtained from their respective oxides RE_2O_3 (RE^{3+}: Y, Eu, Gd and Lu^{3+} – Cstarm, 99.99%) by reaction with concentrated HCl. The aqueous solution of trimesic acid (benzene-1,3,5-tricarboxylic acid – Sigma-Aldrich, 95%) was prepared adding NaOH solution until pH reached ~6.0 [18].

The doped [RE(TMA):Eu^{3+}] complexes (Eu^{3+} concentration of 0.1, 0.5, 1.0 and 5.0 mol%) were prepared by adding 50 mL of $RECl_3$ (~0.050 M) aqueous solution over 200 mL of previously prepared (TMA^{3-}) ligand aqueous solution (~0.0125 M), at temperature of 100 °C for 1 h. The resulting solid was filtered and washed with distilled water, the materials are non-hygroscopic white crystalline powders, air-stable and insoluble in a large range of solvents (ethanol, acetone, acetophenone, benzene, chloroform and DMSO) [14].

Elemental analysis was performed with a Perkin-Elmer CHN 2400 analyzer. The FTIR measurements were made in KBr pellets in a Bomem MB100 FTIR instrument from 400 to 4000 cm^{-1}. Thermogravimetry was performed in a TA HI-RES TGA 2850 equipment from 30 to 900 °C (heating ramp of 5 °C min^{-1}, synthetic air dynamic atmosphere). The XRD patterns were obtained in a Miniflex Rigaku equipment ($CuK_{\alpha 1}$) from 5° to 50° (2θ). The SEM micrographs were recorded in a Field Emission Scanning Electron Microscope model JEOL JSM 7401F, the solid samples were placed on a double-sided copper tape.

The luminescence study was based on the excitation and emission spectra recorded at room (300 K) and liquid nitrogen temperature (77 K). The data was obtained in a SPEX-Fluorolog 2 instrument with double monochromators in front face mode (22.5°) with a 450 W xenon lamp as excitation source. Luminescence decay curves were recorded in a SPEX 1934D phosphorimeter accessory with a 150 W pulsed lamp.

3. Results and discussion

The elemental (Table SI1) and TG analyses [19] of the coordination compounds confirm that the molar ratio between the RE^{3+} ion and TMA ligand is 1:1 with [RE(TMA):Eu^{3+}] anhydrous general formula. On the other hand, the [$Gd(TMA) \cdot (H_2O)_6$:Eu^{3+}(5.0 mol%)] system is the only one that is hydrated with 6 water molecules. The TG analysis of the [RE(TMA):Eu^{3+}] anhydrous materials present no mass-loss event in the temperature range from 30 to 460 °C, except for Gd^{3+}-system (5.0 mol%) that has water loss event from 50 to 150 °C [19]. All the compounds present good thermal stability, corroborating with the elemental analysis data (Table SI1). The thermal behavior indicates the formation of metal-organic framework between the RE^{3+} ions and the TMA ligand. The single-step decomposition event from 460 to 580 °C correspond to the organic moiety decomposition, yielding their respective sesquioxides (RE_2O_3).

The FTIR spectra of the RE^{3+}-complexes (Fig. 1) shows the absorption bands at 1300–1600 cm^{-1} assigned to the TMA ligand symmetric ν_s(C=O) and asymmetric ν_{as}(C=O) stretching modes. The difference $\Delta\nu$ ($\nu_{as} - \nu_s$) for Na_3(TMA) is 195 cm^{-1} and the $\Delta\nu$ values of [RE(TMA):Eu^{3+}] materials are ~175 cm^{-1}, indicating bridge-type coordination [15,20]. Moreover, the narrow absorption peak around 3070 cm^{-1} is assigned to C–H bond stretching characteristic of the anhydrous compounds, which is absent in hydrated [$Gd(TMA) \cdot (H_2O)_6$:Eu^{3+}(5.0 mol%)] complex [14]. The three sharp absorption bands between 690 and 780 cm^{-1} correspond to the out-of-plane C–H bending of the aromatic ring [21]. The infrared absorption spectra (Fig. 1) present similar spectral profile for the doped and undoped anhydrous complexes, except for Gd^{3+}-system (5.0 mol%) corroborated by TG analysis.

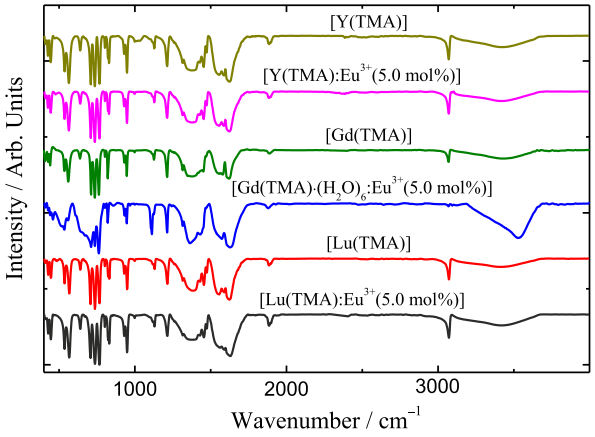

Fig. 1. Infrared spectra of the non-doped and doped [RE(TMA):Eu^{3+}(x mol%)] systems.

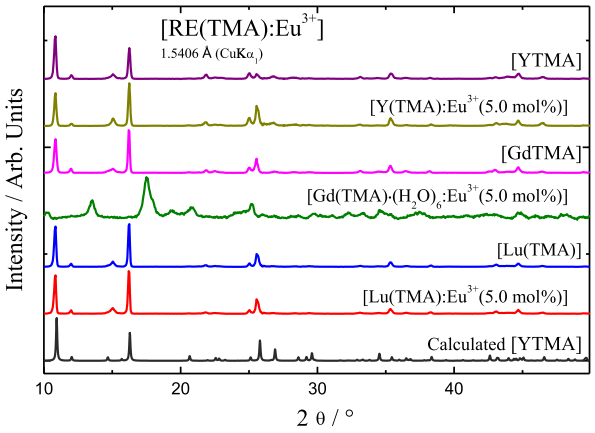

Fig. 2. XRD patterns of the non-doped and doped [RE(TMA):Eu^{3+}(xmol%)] systems.

The powder XRD patterns (Fig. 2) show no relevant difference, in all the anhydrous samples, indicating that the [RE(TMA):Eu^{3+}(x mol%)] can be grouped in one isomorphous series. The patterns are similar to the data for the [RE(TMA)], [RE(TMA):Dy^{3+}] anhydrous complexes reported in the literature [15,22] presenting monoclinic structure (C2/m, no. 12) with centrosymmetric feature.

The similarity in the XRD data suggests that the crystalline structure of the [RE(TMA)] anhydrous complexes presents small perturbation by the doping process indicating the formation of solid solution between the Eu^{3+} dopant and the RE^{3+} in the host matrices due to the comparable radii of these RE^{3+} ions, *Vegard's rule* [23].

The SEM images show the 6–12 μm width and 1 μm thickness sheets-like structure of [Y(TMA):Eu^{3+}(1.0 mol%)] complex (Fig. 3). The images indicate different morphologies compared with the rods reported in Ref. [14] obtained for the hydrated [$Eu(TMA) \cdot (H_2O)_6$] complexes.

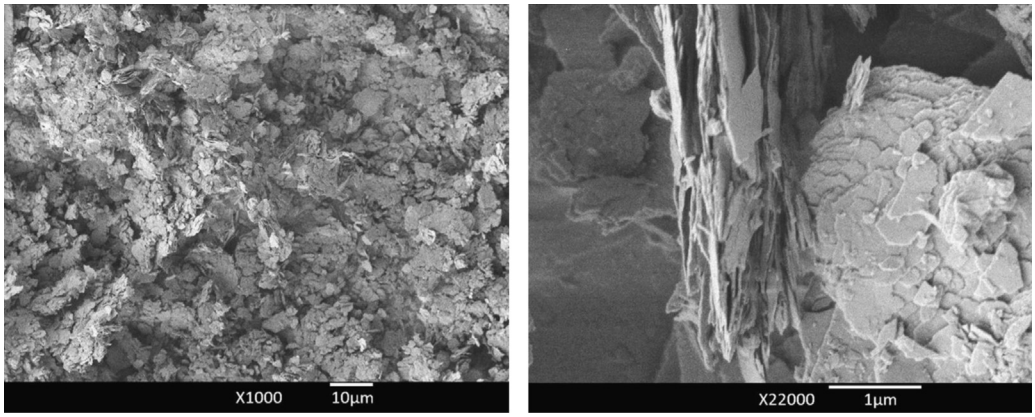

Fig. 3. SEM images of [Y(TMA):Eu^{3+}(1.0 mol%)].

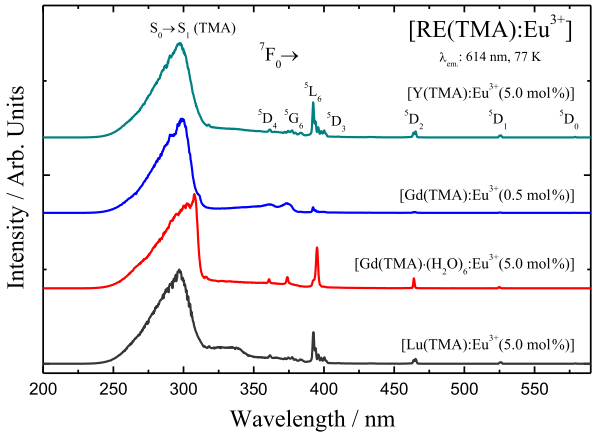

Fig. 4. Excitation spectra of [RE(TMA):Eu^{3+}(*x*mol%)] system recorded at 77 K, monitored at 614 nm.

The excitation spectra of [RE(TMA):Eu^{3+}(*x* mol%)] (RE^{3+}: Y, Gd and Lu) and hydrated Gd^{3+} compounds were monitored at the hypersensitive transition $^5D_0 \rightarrow {}^7F_2$ (614 nm) at 77 K (Fig. 4). The energy levels of the Eu^{3+}-samples were assigned to the absorption bands originated from the ground state $^7F_0$ to the excited levels such as (in cm^{-1}): $^5D_0$ (17,280); $^5D_1$ (19,025); $^5D_2$, (21,530); $^5D_3$ (24,380); $^5L_6$ (25,390); $^5L_7$ (26,475); $^5D_4$ (27,670) (based at the [Y(TMA):Eu^{3+} (5.0 mol%)] compound).

As it can be seen, the $^7F_0 \rightarrow {}^5L_6$ transition (25,390 cm^{-1}) exhibits the highest intensity among the intraconfigurational transitions. The highest intensity of the TMA ligand absorption band is localized in higher energy in the UV region. The efficient energy transfer ligand-to-Eu^{3+} ion is due to the absence of non-radiative decay mediated by water molecules, except for the [Gd(TMA)·$(H_2O)_6$:Eu^{3+}(5.0 mol%)] compound. Besides, the excitation spectra of the [RE(TMA):Eu^{3+}(*x* mol%)] anhydrous compounds show similar profile suggesting that this system present equivalent chemical environment around RE^{3+} ions and optical behaviors.

The emission spectra of the [RE(TMA):Eu^{3+}(*x*mol%)] complexes (RE^{3+}: Y, Gd and Lu) were recorded under excitation in the TMA ligand band (~300 nm) at 77 K, to reduce the vibronic coupling compared to the room temperature (Fig. 5). The emission energy levels of $^5D_0 \rightarrow {}^7F_J$ transitions (J=0–4) of the Eu^{3+} ion can be attributed as the following (in cm^{-1}): $^5D_0 \rightarrow {}^7F_0$ (17,195); $^7F_1$ (16,875); $^7F_2$, (16,190); $^7F_3$ (15,040) and $^7F_4$ (14,215).

The $^5D_0 \rightarrow {}^7F_0$ transition presents only one emission band indicating that the Eu^{3+} ion occupies one symmetry site [24]. The emission spectra show comparable intensities for the hypersensitive transition $^5D_0 \rightarrow {}^7F_2$, allowed by the forced electric dipole and dynamic coupling mechanisms for non-centrosymmetric point groups, and $^5D_0 \rightarrow {}^7F_1$, allowed by magnetic dipole mechanism character [12,21]. The decrease in the phosphorescence intensities of the TMA ligand broad band in the region 420–500 nm with the increase of the Eu^{3+} concentrations indicates that the energy transfer process becomes more efficient [25,26].

Using the emission spectra it is possible to obtain the radiative rates ($A_{0\rightarrow J}$) for the $^5D_0 \rightarrow {}^7F_J$ transitions by Eq. (1) [12,17]

$$A_{0\rightarrow J} = \left(\frac{\sigma_{0\rightarrow 1}}{S_{0\rightarrow 1}}\right)\left(\frac{S_{0\rightarrow J}}{\sigma_{0\rightarrow J}}\right)A_{0\rightarrow 1} \quad (1)$$

where $\sigma_{0\rightarrow 1}$ and $\sigma_{0\rightarrow J}$ correspond to the energy barycenters of the $^5D_0 \rightarrow {}^7F_1$, taken as the reference due to its magnetic dipole character, and $^5D_0 \rightarrow {}^7F_J$ transitions, respectively. The $S_{0\rightarrow 1}$ and $S_{0\rightarrow J}$ are the emission areas of the spectrum corresponding to the $^5D_0 \rightarrow {}^7F_1$ and $^5D_0 \rightarrow {}^7F_J$ transitions, respectively [27]. Since the magnetic dipole $^5D_0 \rightarrow {}^7F_1$ transition is almost insensitive to changes in the chemical environment around the Eu^{3+} ion the $A_{0\rightarrow 1}$ rate can be used as an internal standard to determine the $A_{0\rightarrow J}$ coefficients for Eu^{3+} compounds [17].

The lifetime (τ) of the [RE(TMA):Eu^{3+}(*x* mol%)] materials were obtained from the luminescence decay curve using a mono-exponencial exponential decay. The emission quantum efficiency (η) of the $^5D_0$ emitting level is determined according to Eq. (2)

$$\eta = \frac{A_{\mathrm{rad}}}{A_{\mathrm{rad}} + A_{\mathrm{nrad}}} \quad (2)$$

where the total decay rate, $A_{\mathrm{tot}} = 1/\tau = A_{\mathrm{rad}} + A_{\mathrm{nrad}}$ and the $A_{\mathrm{rad}} = \Sigma_J A_{0\rightarrow J}$. The A_{rad} and A_{nrad} are the radiative and non-radiative rates, respectively. Table 1 shows the experimental values of the radiative (A_{rad}) and non-radiative (A_{nrad}) rates, and emission quantum efficiency (η).

The transitions $^5D_0 \rightarrow {}^7F_2$ and $^5D_0 \rightarrow {}^7F_4$ can be used to estimate the experimental intensity parameters (Ω_λ, λ=2 and 4). The Ω_6 intensity parameter is not included in this study since the $^5D_0 \rightarrow {}^7F_6$ transition was not observed in these materials. The coefficient of spontaneous emission, A, is given by Eq. (3)

$$A_{0\rightarrow J} = \frac{4e^2\omega^3}{3\hbar c^3}\chi \sum_\lambda \Omega_\lambda \langle {}^7F_J \| U^{(\lambda)} \| {}^5D_0 \rangle^2 \quad (3)$$

where, $\chi = n(n+2)^2/9$ is the Lorentz local field correction and n is the refraction index of the medium (1.5 for these materials). The square reduced matrix elements $\langle {}^7F_J \| U^{(\lambda)} \| {}^5D_J \rangle^2$ are 0.0032 and 0.0023 calculated for J=2 and 4, respectively [27,28].

The Ω_λ parameters depend on the local geometry, bonding atom and polarizabilities in the first coordination sphere of metal ion. The three parameters depend equally on the ligating atom

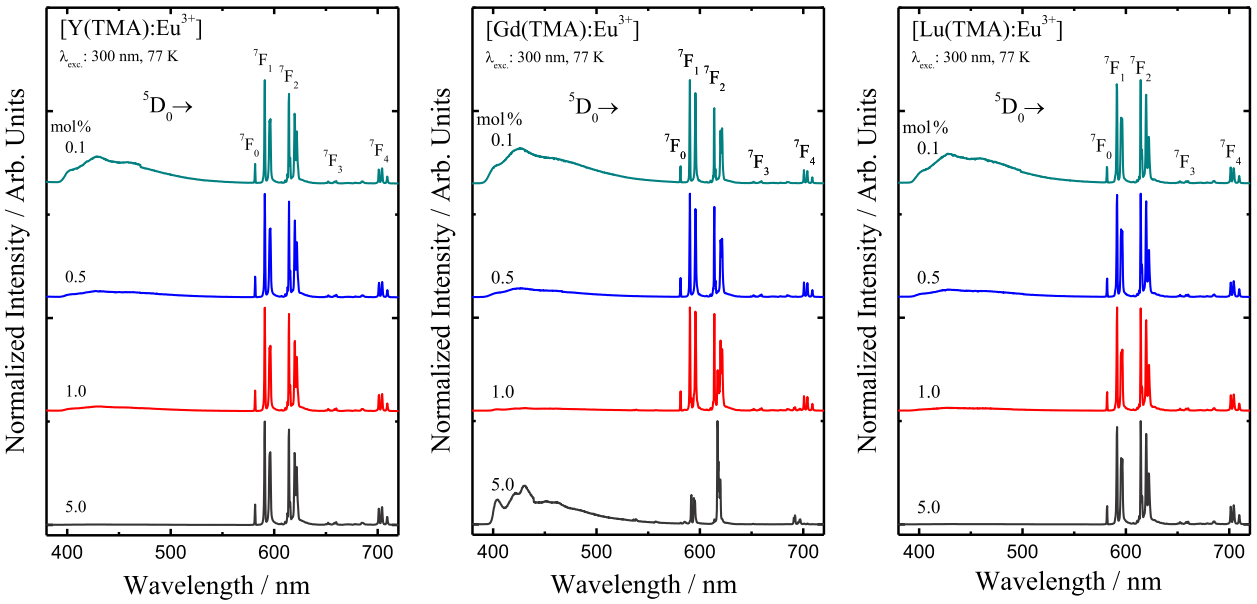

Fig. 5. Emission spectra of the doped [RE(TMA):Eu^{3+}(*x* mol%)] systems recorded at 77 K, under excitation at 300 nm.

Table 1
Experimental intensity parameters ($\Omega_{2,4}$), radiative (A_{rad}), non-radiative (A_{nrad}) and total (A_{tot}) rates, lifetimes of the $^5D_0$ emitting level (τ) and quantum efficiencies (η) for the [RE(TMA):Eu^{3+}(*x* mol%)] materials.

[RE(TMA):Eu^{3+}(*x* mol%)]	Ω_2	Ω_4	A_{rad}	A_{nrad}	A_{tot}	τ	η
	(10^{-20} cm^{-2})	(10^{-20} cm^{-2})	(s^{-1})	(s^{-1})	(s^{-1})	(ms)	(%)
[Y(TMA):Eu^{3+}(0.1)]	2	1	154	202	356	2.81	43
(0.5)	2	1	152	188	339	2.95	45
(1.0)	2	1	155	185	340	2.94	46
(5.0)	2	1	157	204	362	2.76	43
[Gd(TMA):Eu^{3+}(0.1)]	2	2	160	190	348	2.87	46
(0.5)	2	1	155	187	341	2.93	45
(1.0)	2	2	135	249	384	2.60	35
[Gd(TMA)·$(H_2O)_6$:Eu^{3+}(5.0)]	6	3	147	1935	2083	0.73	7
[Lu(TMA):Eu^{3+} (0.1)]	2	1	153	195	348	2.87	44
(0.5)	2	1	156	190	346	2.89	45
(1.0)	2	1	160	182	342	2.92	47
(5.0)	2	1	153	166	320	3.13	48
[Eu(TMA)·$(H_2O)_6$][a]	11	10	623	2015	2637	0.23	12

[a] Ref. [14].

polarizability. However, according to theory, the Ω_2 values are by far the most sensitive to small angular changes in the chemical environment around the Eu^{3+} ion, and it tends rapidly to decrease as the local symmetry tends to a higher one, possibly towards a one with center of inversion.

On the other hand Ω_4 and Ω_6 are by far the most sensitive to ligating atom–metal ion distances, and do not necessarily decrease rapidly as the local symmetry tend to a higher one, possibly towards a one with center of inversion. The Ω_λ ($\lambda=2$ and 4) values for the [RE(TMA):Eu^{3+}(*x* mol%)] compounds ($x=0.1$, 0.5, 1.0 and 5.0 mol%) are presented in Table 1. The Ω_2 values of [RE(TMA)] are much smaller ($\sim 2\cdot 10^{-20}$ cm^{-2}) than that of [Eu(TMA)·$(H_2O)_6$] complex ($\sim 11\cdot 10^{-20}$ cm^{-2}) [14], agreeing with the crystallography data [21], which show that the anhydrous complex tends to a point group with inversion center [29,30]. Thus, these theoretical considerations might be used to rationalize the Ω_λ behaviors in Table 1.

The lifetime values (~2.90 ms) presented by the [RE(TMA):Eu^{3+}(*x* mol%)] phosphors are longer than for the majority of the Eu^{3+}-complexes reported in the literature [14,17] and one order of magnitude higher than the [Eu(TMA)·$(H_2O)_6$] (0.23 ms) and three times higher than the [Gd(TMA)·$(H_2O)_6$:Eu^{3+}(5.0 mol%)] (0.73 ms). This optical property corroborates that the absence of water molecules is very important, as indeed expected, to the photoluminescence efficiency, avoiding the luminescence quenching, due the non-radiative decay pathways mediated by vibrational levels of the O–H oscillators.

The emission quantum efficiency values of the anhydrous compounds ($\eta\sim 45\%$) are higher than for [Eu(TMA)·$(H_2O)_6$] ($\eta=12\%$) and [Gd(TMA)·$(H_2O)_6$:Eu^{3+}(5.0 mol%)] ($\eta=7\%$) complexes confirming that the water molecules are responsible to the luminescence quenching for the hydrated compounds (Table 1) [14]. Moreover, the increase in the Eu^{3+} concentration from 0.1 to 5.0 mol% does not affect the emission quantum efficiency suggesting that the luminescence quenching concentration effect is not operative.

The color coordinates of the complexes in the CIE chromaticity diagram (*Commission Internationale de l'Eclairage*) are shown in Fig. 6 (left) [31]. The color purity increases with the raise of Eu^{3+}-doping concentration (0.651, 0.337 for [Y(TMA):Eu^{3+}(5.0 mol%)]). The [RE(TMA):Eu^{3+}(*x* mol%)] crystalline powder samples emits an intense red light, when irradiated with light in the ultraviolet region Fig. 6 (right).

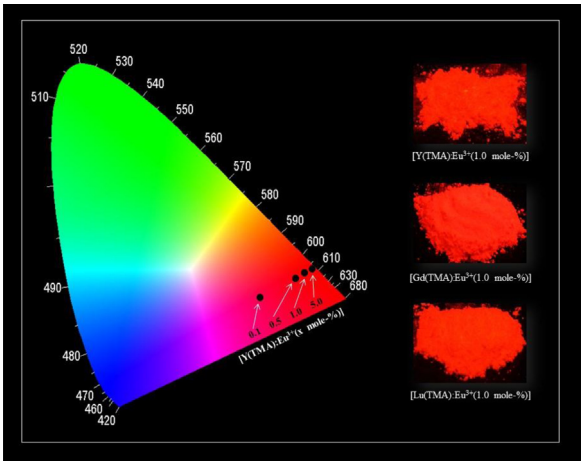

Fig. 6. CIE chromaticity diagram showing the *x*,*y* emission color coordinates for [Y(TMA):Eu^{3+}(*x* mol%)] (*x*: 0.1 (left), 0.5, 1.0 and 5.0 (right)) and picture of [RE(TMA):Eu^{3+} (1.0 mol%) (RE^{3+}: Y, Gd and Lu), irradiated at 254 nm. (For interpretation of the references to color in this figure, the reader is referred to the web version of this article.)

4. Conclusion

The highly efficient anhydrous red emitting [RE(TMA):Eu^{3+}] materials were prepared by a one-step synthesis in aqueous solution. The TG curves show the absence of water molecules in the structure, thermostability up to 460 °C and single-step decomposition of the organic moiety. The XRD data indicate an isostructural series for the anhydrous complexes. The TMA ligand T_1 state has higher energy than the $^5D_0$ (Eu^{3+}) emitting level, acting as intramolecular energy transfer donor to the Eu^{3+} ion. The [RE(TMA):Eu^{3+}] anhydrous compounds present monochromatic red emission and quantum efficiency at around 45%. The small values of the Ω_2 and Ω_4 parameters for the anhydrous compounds corroborates with a local point symmetry and also a rather low polarizability around the Eu^{3+} ion, respectively. Photoluminescence data show that these materials can act as an efficient red light conversion molecular devices (LCMDs) and the lowest Eu^{3+}-concentration doped compounds can be used as efficient and more economically viable optical markers.

Acknowledgments

The authors acknowledge financial support from Conselho Nacional de Desenvolvimento Científico e Tecnológico (CNPq - Project Number: 482117/2009-5), Coordenação de Aperfeiçoamento de Pessoal de Nível Superior (CAPES - Project Number: 078/2009/DBP) Fundação de Amparo à Pesquisa do Estado de São Paulo (FAPESP - Project Number: 03/07178-8) and Nanobiotec-Brasil-RH-INAMI and inct-INAMI (Project Number: 57.3986-2008-8).

Appendix A. Suplementary information

Supplementary data associated with this article can be found in the online version at http://dx.doi.org/10.1016/j.jlumin.2015.04.047.

References

[1] A. Battaglia, C. Bertucci, E. Bombardelli, S. Cimitan, A. Guerrini, P. Morazzoniand, A. Riva, Eur. J. Med. Chem. 38 (2003) 383.
[2] J. Rocha, L.D. Carlos, F.A.A. Paz, D. Ananias, Chem. Soc. Rev. 40 (2011) 926.
[3] S. Stepanow, M. Lingenfelder, A. Dmitriev, H. Spillmann, E. Delvigne, N. Lin, X. Deng, C. Cai, J.V. Barth, K. Kern, Nat. Mater. 3 (2004) 229.
[4] J. Della Rocca, D. Liu, W. Lin, Acc. Chem. Res. 44 (2011) 957.
[5] S. Sugimoto, J. Phys. D: Appl. Phys. 44 (2011) 064001.
[6] H. Ma, J. Okuda, Macromolecules 38 (2005) 2665.
[7] V.S. Sastri, J.C. Bunzli, J.R. Perumareddi, V.R. Rao, G.V.S. Rayudu, Modern Aspects of Rare Earths and their Complexes, Elsevier, Amsterdam, 2003.
[8] J. Kido, Y. Okamoto, Chem. Rev. 102 (2002) 2357.
[9] J. Hölsä, T. Laamanen, M. Lastusaari, M. Malkamäki, P. Novák, J. Lumin. 129 (2009) 1606.
[10] P. Gawryszewska, J. Sokolnicki, J. Legendziewicz, Coord. Chem. Rev. 249 (2005) 2489.
[11] K. Binnemans, Chem. Rev. 109 (2009) 4283.
[12] G.F. de Sá, O.L. Malta, C.M. Donega, A.M. Simas, R.L. Longo, P.A. Santa-Cruz, E.F. Silva Jr., Coord. Chem. Rev. 196 (2000) 165.
[13] N. Sabbatini, M. Guardigli, J.M. Lehn, Coord. Chem. Rev. 123 (1993) 201.
[14] E.R. Souza, I.G.N. Silva, E.E.S. Teotonio, M.C.F.C. Felinto, H.F. Brito, J. Lumin. 130 (2010) 283.
[15] I.G.N. Silva, J. Kai, M.C.F.C. Felinto, H.F. Brito, Opt. Mater. 35 (2013) 978.
[16] M.A. Guedes, T.B. Paolini, M.C.F.C. Felinto, J. Kai, L.A.O. Nunes, O.L. Malta, H.F. Brito, J. Lumin. 131 (2011) 99.
[17] H.F. Brito, O.L. Malta, M.C.F.C. Felinto, E.E.S. Teotonio, The Chemistry of Metal Enolates, Luminescence Phenomena Involving Metal Enolates, John Wiley & Sons, England, 2009.
[18] H.C. Brown, D.H. McDaniel, O. Häfligler, F.C. Nachod, E.A. Braude, Determination of Organic Structures by Physical Methods, New York Academic Press, New York, 1962.
[19] I.G.N. Silva, L.C.V. Rodrigues, E.R. Souza, J. Kai, M.C.F.C. Felinto, J. Hölsä, H.F. Brito, O.L. Malta, Opt. Mater. 40 (2015) 41.
[20] K. Nakamoto, Infrared and Raman Spectra of Inorganic and Coordination Compounds, John Wiley & Sons, New York, 1997.
[21] R. Lyszczek, J. Therm. Anal. Calorim. 90 (2007) 533.
[22] C. Serre, F. Millange, C. Thouvenot, N. Gardant, F. Pellé, G. Férey, J. Mater. Chem. 14 (2004) 1540–1543.
[23] L. Vegard, Z. Phys. 5 (1921) 17.
[24] P.P. Lima, S.S. Nobre, R.O. Freire, S.A. Jr., R.A. Sá Ferreira, U. Pischel, O.L. Malta, L.D. Carlos, J. Phys. Chem. C 111 (2007) 17627.
[25] O.L. Malta, H.F. Brito, J.F.S. Menezes, F.R.G. Silva, S. Alves Jr., F.S. Farias Jr., A.V.M. de Andrade, J. Lumin. 75 (1997) 255.
[26] F.R.G.E. Silva, O.L. Malta, J. Alloy. Compd. 250 (1997) 427.
[27] E.E.S. Teotonio, G.M. Fett, H.F. Brito, W.M. Faustino, G.F. de Sá, M.C.F.C. Felinto, R.H.A. Santos, J. Lumin. 128 (2008) 190.
[28] L.D. Carlos, Y. Messaddeq, H.F. Brito, R.A. Sá Ferreira, V.Z. Bermudez, S.J.L. Ribeiro, Adv. Mater. 12 (2000) 594.
[29] R.A. Sá Ferreira, S.S. Nobre, C.M. Granadeiro, H.I.S. Nogueira, L.D. Carlos, O.L. Malta, J. Lumin. 121 (2006) 561.
[30] I.G.N. Silva, H.F. Brito, E.R. Souza, D. Mustafa, M.C.F.C. Felinto, L.D. Carlos, O.L. Malta, Z. Naturforschung B 69b (2014) 231.
[31] P.A. Santa-Cruz, F.S. Teles, Spectra Lux Software v.2.0 Beta, Ponto Quântico Nanodispositivos, RENAMI, 2003.